A comparison of MR sequences for lesions of the parotid gland.

M J Sharafuddin, D P Diemer, R S Levine, J L Thomasson and A L Williams

AJNR Am J Neuroradiol 1995, 16 (9) 1895-1902
http://www.ajnr.org/content/16/9/1895

A Comparison of MR Sequences for Lesions of the Parotid Gland

Melhem J. A. Sharafuddin, David P. Diemer, Richard S. Levine, Jeffrey L. Thomasson, and Allan L. Williams

PURPOSE: To compare six MR sequences (plain and gadolinium-enhanced fat suppressed T1-weighted spin echo, T2-weighted standard spin echo, fat-suppressed and non–fat-suppressed T2-weighted fast spin echo, and inversion-recovery T2-weighted fast spin echo) in their ability to detect, delineate, and characterize lesions of the parotid gland. **METHODS:** Fifty-eight parotid gland lesions imaged on 47 examinations were retrospectively evaluated by three blinded observers. Several outcome-related variables were compared by the above six sequences: imaging time, image quality, anatomic sharpness of parotid space, subjective lesion conspicuity, detected abnormality volume, number of individual lesions or discrete lobulations, conspicuity of invasion into adjacent boundaries and structures, and overall diagnostic value. **RESULTS:** Differences in the above outcome variables between sequences did not correlate with MR scanner software upgrade level, coil type, or lesion-dependent characteristics. Fat-suppressed fast spin-echo T2-weighted and inversion-recovery fast spin-echo T2-weighted sequences resulted in significantly higher scores for lesion conspicuity, detected abnormality volume, and overall diagnostic value. T1-weighted images resulted in the next highest scores, whereas gadolinium-enhanced T1-weighted and standard spin-echo T2-weighted sequences performed poorly for most parotid lesions. **CONCLUSION:** MR imaging of the parotid gland should include fat-suppressed, long-repetition-time, fast spin-echo T2-weighted, and T1-weighted sequences. Gadolinium-enhanced images need not be obtained routinely.

Index terms: Salivary glands, magnetic resonance; Magnetic resonance, comparative studies

AJNR Am J Neuroradiol 16:1895–1902, October 1995

Magnetic resonance (MR) imaging is a premiere imaging modality for the evaluation of parotid gland masses (1–14). The value of fast spin-echo sequences and fat suppression in the imaging of extracranial head and neck lesions has been reported (1, 2, 8, 11, 12, 15). In the parotid gland, because of the normally high fat content, contrast between normal tissue and disease can be low on T2-weighted images, especially with fast spin-echo sequences. We retrospectively analyzed our experience with a wide range of parotid gland lesions and compared standard spin-echo and fat-suppressed fast spin-echo sequences, attempting to arrive at useful guidelines for MR imaging of parotid gland masses.

Material and Methods

Patients

All parotid gland lesions imaged at one institution since late 1990 were retrospectively analyzed. Six examinations (in 4 patients) were eliminated from the study because of inappropriate windowing, gross artifact, or compromised image quality on more than one sequence. A total of 58 lesions imaged on 47 examinations were evaluable for the study. There were 31 female and 16 male subjects, with a mean age of 42 years (range, 7 to 70 years). The lesion categories included benign neoplasms (n = 21), malignant neoplasms (n = 6), multiple or metastatic neoplasms (n = 9), inflammatory conditions (n = 11), cystic lesions (n = 6), lipomatous lesions (n = 4), and hemangioma (n = 1).

Presented in part at the American Roentgen Ray Society 95th Annual Meeting, New Orleans, La, 1994.

Received February 17, 1995; accepted after revision May 16.

From the Department of Radiology, St Louis (Mo) University Health Sciences Center (M.J.A.S., D.P.D., R.S.L., J.L.T., A.L.W.) and the Department of Radiology, St John's Mercy Medical Center, St Louis, Mo (D.P.D., R.S.L., J.L.T.).

Address reprint requests to M. J. A. Sharafuddin, MD, Department of Radiology, St Louis University Health Sciences Center, 3635 Vista Ave at Grand Blvd, St Louis, MO 63110–0250.

AJNR 16:1895–1902, Oct 1995 0195-6108/95/1609–1895

MR Imaging

Six sequences were used in various combinations: plain T1-weighted spin-echo, fat-suppressed gadolinium-enhanced T1-weighted spin-echo (Gd T1), standard spin-echo T2-weighted (SSE T2), and fast spin-echo T2-weighted images with and without fat suppression (FS FSE T2 and FSE T2, respectively). We also began using inversion recovery fast spin-echo T2-weighted images (IR FSE T2) in late 1993.

Two 1.5-T signa units, software levels from 4.8 to 5.2 (General Electric, Milwaukee, Wis) were used. Either a quadrature head coil or a receive-only volume cervical coil was used. Images were obtained in 5-mm-thick sections with 1-mm intersection gap. T1-weighted imaging parameters were 550-650/10-15/1 (repetition time/echo time/excitations), with 256 × 192 matrix. T2-weighted imaging parameters on spin-echo sequences were 2000-2500/20-80/0.75-1, superior and inferior saturation pulses, with 256 × 192 matrix. T2-weighted imaging parameters on fast spin echo sequences were 5000-6000/119 (effective)/2-4; echo train length, 119; single echo, superior, and inferior saturation pulses; image matrix varying from 256 × 192 to 512 × 256. Fat suppression in FS FSE T2 and in most gadolinium-enhanced images was achieved by the frequency-selective, chemical-presaturation method. The other fat-suppressed T2-weighted sequence was IR FSE T2, with the parameters 4000-6000/26-85/1; 256 × 192 matrix; and 140 to 170 inversion time. For all images, window/level settings were carefully adjusted by experienced MR imaging technologists to optimize tissue contrast in the parotid space.

Analysis of MR Imaging Data

The images were analyzed by three investigators who were blinded to the diagnosis but not to the MR imaging sequence. Weighted κ statistics showed good interobserver congruency.

Designated Variables

Several outcome-related variables were derived for each lesion and individually scored by each observer for each sequence used in the examination. Time taken to complete a 12-section series was expressed in seconds. Image quality, regardless of the diagnostic value, was subjectively scored. The anatomic sharpness, related to the definition of anatomic contents and boundaries of the parotid space, was subjectively scored. The subjective conspicuity of abnormality, relative to the surrounding tissue, also was scored. Subjective conspicuity has been found elsewhere to closely reflect the measured lesion contrast-to-noise ratio (16, 17). Abnormality volume was ranked according to the subjective size of abnormality detected on one sequence, relative to the remaining sequences. The number of individual lesions or discrete lobulations within one lesion was determined for multifocal, or lobulated, lesions. For invasive lesions, conspicuity of the invasion into adjacent boundaries and structures also was subjectively scored. The overall value of each sequence also was subjectively graded in terms of the value of the sequence in assisting the diagnosis. All subjective scores varied from 1 to 5 (poor to excellent).

Lesion-related variables (sequence-independent) also were derived for each lesion, including category, size, margination, signal homogeneity, and, when applicable, the degree and pattern of enhancement. Equipment-related variables including software upgrade level of the MR scanner and coil type also were recorded.

Statistical Analysis

Outcome variables (imaging time, quality, sharpness, conspicuity, invasion, number, and overall value) were compared in the six sequences (T1, Gd T1, SSE T2, FS FSE T2, FSE T2, IR FSE T2) using one-way analysis of variance (ANOVA) and Kruskal-Wallis nonparametric ANOVA. Least significance difference-multiple range test was used for paired comparison of imaging time by sequence. Mann-Whitney/Wilcoxon's rank sum test was used for paired comparison of nonparametric variables by sequence. When comparing small groups containing fewer than 10 cases, a significance threshold of $P < .1$ was used, otherwise $P < .05$ was used.

The sequences also were compared for certain specific lesion categories including cystic, lipomatous, small (≤10 mm), and large (≥2 cm). Comparison was limited to T1, Gd T1, and FS FSE T2 sequences because of insufficient number of cases imaged with other sequences.

Correlation analysis was performed between three outcome variables (conspicuity, volume, and overall value) and five categorizing variables (upgrade, coil, quality, size, and enhancement).

Results

Imaging time, subjective lesion conspicuity, anatomic sharpness in the parotid space, overall diagnostic value, and number of individual lesions detected were all significantly dependent on the MR imaging sequence. These variables were, however, unrelated to software upgrade level, coil type, image quality, or lesion-related characteristics (such as lesion category, size, borders, signal homogeneity, and enhancement). Paired comparison of outcome-based variables by MR imaging sequences is summarized in Tables 1 and 2.

Imaging time was significantly shorter with both FSE T2 and FS FSE T2 sequences compared with the remaining sequences. Mean imaging time was shortest for FSE T2 and longest for Gd T1.

TABLE 1: The diagnostic value of analyzed MR imaging sequences, expressed in mean rank scores, for each of the analyzed outcome variables

	Quality	Sharpness	Conspicuity	Volume	Number*	Invasion†	Overall
FS FSE T2	88 (43)	90 (43)	106 (n = 43)	100 (n = 43)	25 (n = 10)	20 (n = 5)	109 (n = 43)
IR FSE T2	96 (6)	69 (6)	114 (n = 6)	106 (n = 6)	. . .	. . .	102 (n = 6)
FSE T2	86 (9)	96 (9)	79 (n = 9)	77 (n = 9)	6 (n = 1)	14 (n = 1)	81 (n = 9)
T1	85 (52)	88 (52)	83 (n = 52)	79 (n = 52)	17 (n = 10)	12 (n = 10)	79 (n = 52)
Gd T1‡	80 (43)	77 (43)	64 (n = 43)	73 (n = 43)	9 (n = 9)	13 (n = 6)	66 (n = 43)
SSE T2	70 (13)	64 (13)	67 (n = 13)	75 (n = 13)	15 (n = 2)	9 (n = 4)	66 (n = 13)

Note.—n indicates cases per sequence.
* Multiple or multilobulated lesions only.
† Invasive lesions only.
‡ Fat suppression used in most cases.

The highest image quality scores were achieved by FS FSE T2 and IR FSE T2 sequences although the only statistically significant difference was between FS FSE T2 and SSE T2 sequences. The anatomic sharpness in the parotid space was significantly better with FS FSE T2 images than with IR FSE T2, SSE T2, and T1 Gd images.

Parotid gland disease was most conspicuous on FS FSE T2 and IR FSE T2 images, with significantly higher mean rank scores than the other sequences (Fig 1). Although IR FSE T2 mean rank was higher than FS FSE T2, the difference between the two scores was not statistically significant ($P = .73$). The next highest conspicuity was achieved by T1, with significantly higher mean rank score than Gd T1, FSE T2, and SSE T2 images. The volume of abnormality also was best depicted on FS FSE T2 and IR FSE T2 images (highest relative size of de-

TABLE 2: Ranking and significant differences of MR imaging sequences (expressed in mean rank scores) for each of the analyzed outcome variables

	Mean Rank Score (in Decreasing Order)	Statistically Significant Differences§
Overall	FS FSE T2 > IR FSE T2 > FSE T2 > T1 > Gd T1 > SSE T2	FS FSE > [SSE T2$^{(c)}$/Gd T1$^{(d)}$/T1$^{(d)}$/FSE T2$^{(b)}$] IR FSE T2 > [SSE T2$^{(b)}$/Gd T1$^{(b)}$/T1$^{(a)}$]
Sharpness	FSE T2 > FS FSE T2 > T1 > Gd T1 > IR FSE T2 > SSE T2	FS FSE T2 > [Gd T1$^{(b)}$/SSE T2$^{(c)}$/IR FSE T2$^{(a)}$]
Imaging time	FSE T2 > FS FSE T2 > T1 > IR FSE T2 > SSE T2 > Gd T1	FS FSE T2 and FSE T2 < [T1$^{(b)}$/IR FSE T2$^{(b)}$/SSE T2$^{(b)}$/Gd T1$^{(b)}$]
Conspicuity	IR FSE T2 > FS FSE T2 > T1 > FSE T2 > SSE T2 > Gd T1	FS FSE T2 > [Gd T1$^{(d)}$/SSE T2$^{(c)}$/FSE T2$^{(a)}$/T1$^{(c)}$] IR FSE T2 > [Gd T1$^{(b)}$/SSE T2$^{(a)}$/T1$^{(a)}$] T1 > Gd T1$^{(b)}$
Volume	IR FSE T2 > FS FSE T2 > T1 > FSE T2 > SSE T2 > Gd T1	FS FSE T2 > [Gd T1$^{(c)}$/T1$^{(c)}$] IR FSE T2 > Gd T1$^{(a)}$
Number*†	FS FSE T2 > T1 > SSE T2 > Gd T1 > FSE T2	FS FSE T2 > [Gd T1$^{(b)}$/SSE T2$^{(a)}$] T1 > [FSE T2$^{(a)}$/Gd T1$^{(a)}$/SSE T2$^{(a)}$]
Invasion*‡	FS FSE T2 > FSE T2 > T1 > Gd T1 > SSE T2	FS FSE T2 > [SSE T2$^{(b)}$/T1$^{(a)}$/Gd T1$^{(b)}$]

* Insufficient cases for analysis of number and invasion with IR FSE.
† Multiple or multilobulated lesions only.
‡ Invasive lesions only.
§ Significance levels are $^{(a)}$ $P < 0.1$; $^{(b)}$ $P < 0.05$; $^{(c)}$ $P < 0.01$; and $^{(d)}$ $P < 0.001$.

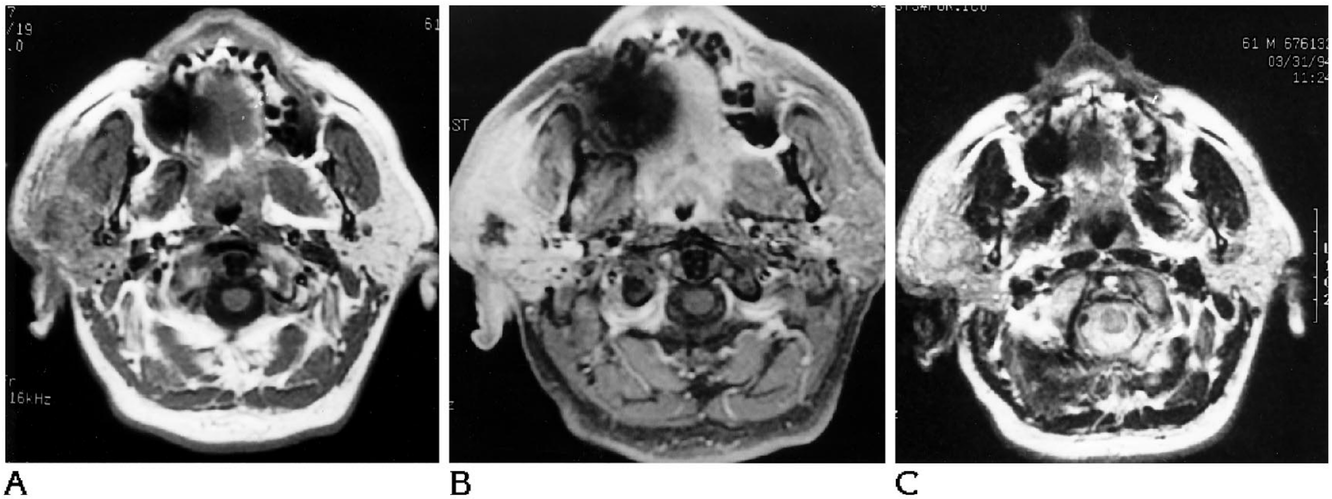

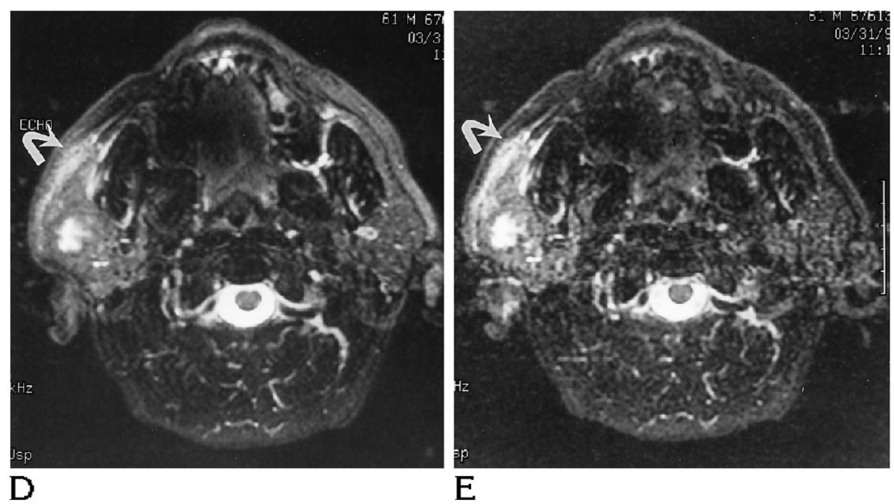

Fig 1. Right-sided parotitis with an intraparotid abscess in a 61-year-old man. MR imaging of the parotid in five different sequences: (*A*) T1-weighted (T1), (*B*) gadolinium-enhanced fat-suppressed T1-weighted (Gd T1), (*C*) standard spin-echo T2-weighted (SSE T2), (*D*) fat-suppressed T2-weighted FSE (FS FSE T2), and (*E*) inversion recovery fast spin-echo (IR FSE T2). There is swelling and diffuse edema of the right parotid gland, with T1 and T2 prolongation, and a central area of liquefaction representing an intraparotid abscess. Superior subjective conspicuity (perceived contrast-to-noise ratio) is evident on FS FSE T2 and IR FSE T2 images compared with SSE T2 and T1 images. The Gd T1 image is helpful in delineating liquefaction corresponding to the intraparotid abscess. Inflammatory edema (*curved arrow*) is better demonstrated on the FS FSE T2 and IR FSE T2 images.

tected abnormality), with FS FSE T2 score being significantly higher than T1, Gd T1, and SSE T2 (Fig 2). When the conspicuity in visualizing invasion was compared (for invasive lesions), FS FSE T2 showed invasion significantly better than the remaining sequences. For multiple and lobulated lesions, both FS FSE T2 and T1 sequences showed significantly more individual lesions or lobulations per parotid gland (Fig 3). IR FSE T2 images could not be analyzed for number of lesions and invasion because of insufficient number of cases. The highest overall diagnostic value was achieved by FS FSE T2 and IR FSE T2 sequences with significantly higher mean rank scores with FS FSE T2 than with all other sequences, with the exception of IR FSE T2.

In the category of cysts and cystic lesions, FS FSE T2 and Gd T1 sequences generally resulted in the highest conspicuity and overall value scores. For lipomatous lesions, T1 sequences achieved the highest conspicuity, overall value, and volume scores. For lesions smaller than 1 cm, as well as those greater than 2 cm, FS FSE T2 sequences resulted in the highest mean rank scores for conspicuity, volume and overall diagnostic value.

Both image quality and anatomic sharpness achieved in the parotid space showed a weak correlation with the software upgrade level ($r = .26$ and $.28$; $P < .1$). Conspicuity, abnormality volume, and overall diagnostic value did not significantly correlate with software level or coil

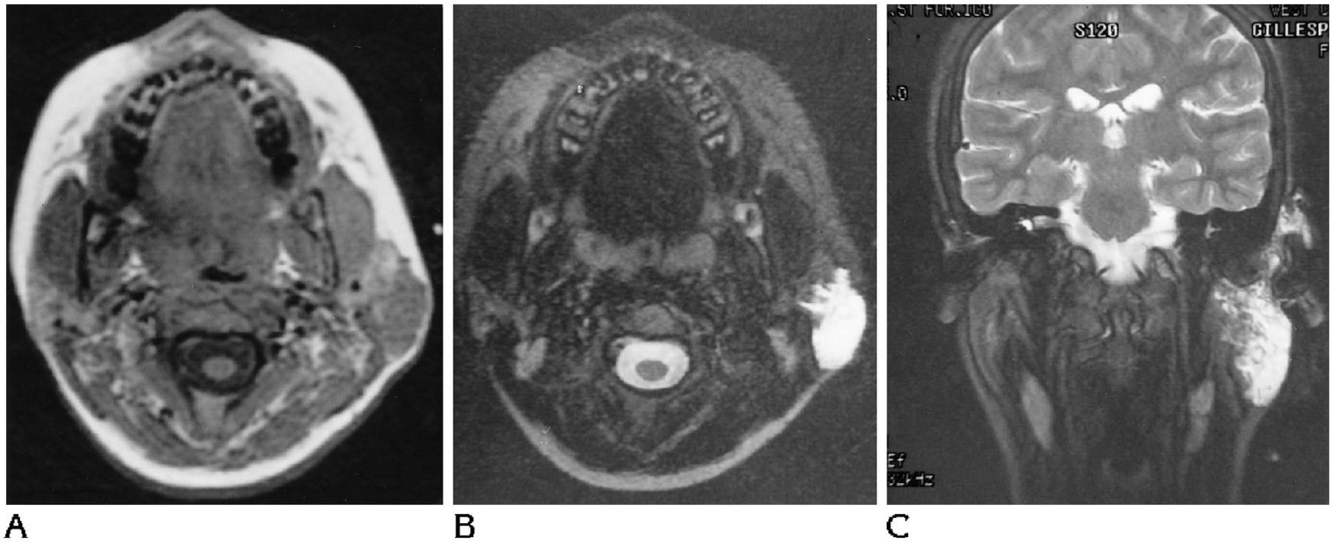

Fig 2. Parotid hemangioma in a 9-year-old girl.

A, Axial T1-weighted and *B*, *C*, axial and coronal fat-suppressed T2-weighted fast spin echo (FS FSE T2) images show an infiltrative lesion with T2 prolongation and involvement of adjacent skin and external ear. Conspicuity and extent of abnormality are much better depicted on the FS FSE T2 images.

type. Lesion conspicuity correlated well with the volume of abnormality ($r = .72$; $P < .01$).

Discussion

The recent introduction of fast spin-echo sequences has been a significant development in MR imaging (6). Fast spin-echo images offer several advantages over traditional sequences, including substantial decrease is imaging time, improved patient tolerance, and reduced motion and magnetic susceptibility artifacts (6, 9). Although the T2-weighted contrast on fast spin echo sequences is very similar to that on standard spin-echo sequences, an important difference is the persistence of bright fat signal on fast spin-echo images. This is thought to be the result of decreased J coupling attributable to the multiple 180° refocusing pulses (18). The other difference is the reduction of magnetic susceptibility artifact, which is advantageous for imaging soft tissue regions adjacent to bone and dental fillings. However, this can result in obscuration of small foci of hemosiderin and cal-

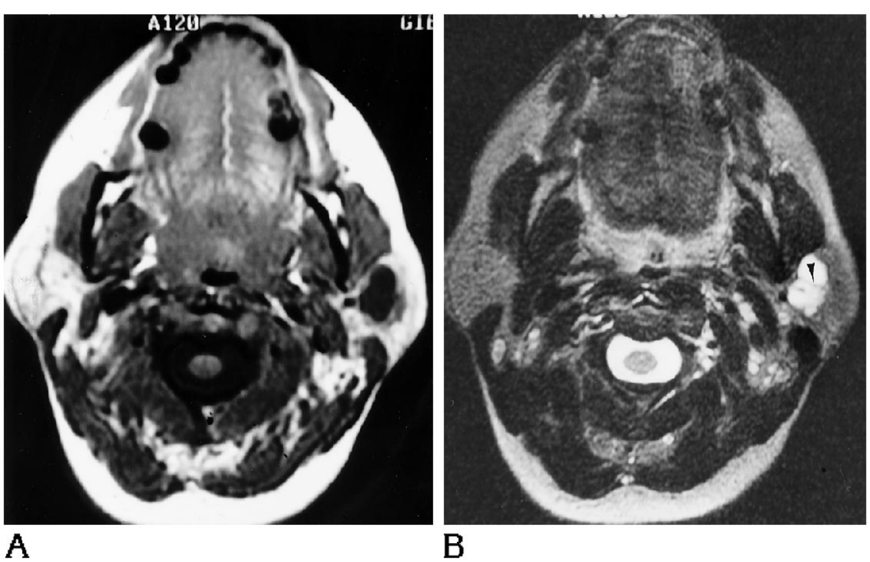

Fig 3. Pleomorphic adenoma of the parotid in a 45-year-old woman.

A, T1-weighted and *B*, fat-suppressed T2-weighted fast spin-echo (FS FSE T2) images. The FS FSE T2 image shows multiple internal septations and lobulations (*arrowhead*) not seen on the T1-weighted image.

cium, which can further compromise the capability to detect salivary calculi and phleboliths on MR imaging (6). Clinical experience with fast spin-echo has shown its value in the central nervous system orbits, head and neck, musculoskeletal system, and abdomen and pelvis (1, 9, 11, 16, 17, 19–22). In the head and neck, T2-weighted fast spin echo images have resulted in improved conspicuity and increased number of detected individual lesions even without the use of fat suppression (11, 23). Another report, however, found no significant difference between fat-suppressed T2-weighted fast spin echo and T2-weighted standard spin echo images in head and neck tumors (1).

The abundance of fat in the parotid space necessitates the use of fat suppression with T2-weighted fast spin-echo sequences to preserve contrast between intraparotid lesions and normal gland (10, 15). Suppression of the bright fat signal also results in expansion of the gray scale dynamic range and decreased motion artifact, which translates into improved conspicuity of regions of abnormal T2 prolongation. The value of fat suppression in head and neck lesions has been clinically demonstrated (1, 2, 4, 6–8, 10, 12, 15, 24) (Vogl T, Mack MJ, Juergens M, et al, “MR Imaging with High-Dose Gadolamide Injection of the Head and Neck: Results in a Phase III Trial and Comparison with the Use of Standard-Dose Gd-DTPA,” *Radiology* 1993; 189[P]:107 [abstr]). Fat suppression also has been shown to improve visualization of gadolinium enhancement on T1-weighted sequences (1, 6, 24). The most widely used fat suppression method is frequency-selective or chemical presaturation (6). Short-inversion-time inversion recovery is another popular fat-suppression sequence that has been reported to be advantageous in the imaging of parotid gland legions, although no comparison group or statistical analysis was presented (12). A drawback of the chemical-presaturation method is its liability to bulk-susceptibility and magnetic-susceptibility artifacts, resulting in asymmetric fat suppression, which may obscure or falsely mimic disease (6, 25). Inversion-recovery fast spin-echo sequences also have been recently described, offering reliable fat suppression substantially faster than with standard short-inversion-time inversion recovery sequences (2, 18).

In our experience FS FSE T2 sequences resulted in significant reduction in imaging time compared with Gd T1, T1, SSE T2, and IR FSE T2 sequences, despite two to four times more signal averages and higher-resolution matrices. FS FSE T2 sequences also resulted in the highest anatomic sharpness in the parotid space, partly because of the ability to use a higher-resolution matrix without prolongation of imaging time. FS FSE T2 sequences, along with IR FSE T2 sequences, also resulted in the highest lesion conspicuity and overall diagnostic value. Moreover, FS FSE T2 and IR FSE T2 images resulted in the visualization of a relatively larger volume of abnormality compared with other sequences. However, in the absence of a standard to measure the actual lesion size in our study, this observation does not necessarily indicate that FS FSE T2 provides a more accurate assessment of tumor size (unfortunately, abnormality size on MR could not be correlated with direct pathologic measurement of abnormality size, given the retrospective nature of the study). FS FSE T2 resulted in an improved conspicuity of invasion (for invasive lesions) and detected more individual lesions or lobulations (for multiple or multilobulated lesions). Although the small number of cases did not permit statistical analysis, a general tendency of FS FSE T2 to outperform T1 and Gd T1 sequences was noted for both very small and large lesions. In addition, both FS FSE T2 and Gd T1 appeared superior to T1 for cystic lesions. However, for lipomatous lesions, T1 appeared more advantageous than FS FSE T2.

Our limited experience with IR FSE T2 has been quite satisfactory. IR FSE T2, along with FS FSE T2, resulted in the highest outcome scores and not infrequently achieved higher scores than FS FSE T2. However, differences were statistically less significant, probably reflecting the smaller number of cases (6 cases imaged with IR FSE T2, compared with 43 cases imaged with FS FSE T2). We have found IR FSE T2 to be extremely sensitive to pathology and provide more reliable and uniform fat suppression than with chemical presaturation. Drawbacks of this sequence included reduced anatomic sharpness in the parotid space and longer acquisition time. Recently, in a study of 46 lesions of the head and neck (of which only a few occurred in the parotid), lesion conspicuity was improved with IR FSE T2 compared with FSE T2 images in 48% of cases, the majority of which were small lesions and lesions surrounded by fat (2).

T1-weighted images generally resulted in good outcome scores, although the ranks were frequently lower than for FS FSE T2 and IR FSE T2 images. We believe T1-weighted images always should be a part of the parotid examination and, certainly, should not be replaced by gadolinium-enhanced T1-weighted images. T1-weighted images, although providing good lesion conspicuity and better anatomic details outside the parotid space, also are diagnostically helpful for tissue characterization in lipid-containing lesions, cysts, hemorrhage, and lesions rich in melanin (melanotic melanoma).

Despite the reported value of gadolinium-enhanced sequences for MR imaging of head and neck lesions in general (7, 24) (Vogl T et al., "MR Imaging with High-Dose . . ."), we have found it to be of limited value in the imaging of parotid masses. We believe this to be related to simultaneous enhancement of both tumor and normal parotid parenchyma resulting in decreased lesion conspicuity on the enhanced images. Decreased delineation of fat planes on gadolinium-enhanced T1-weighted images also may result in loss of anatomic details and poor demarcation of the various anatomic compartments. Nevertheless, gadolinium-enhanced T1-weighted images have been reported to be helpful in the diagnosis of Warthin tumor, which frequently does not enhance (5). In our experience with 4 Warthin tumors, 3 showed no enhancement, and one only enhanced minimally, whereas minimal or no enhancement occurred in only 2 of 24 other well-marginated benign and malignant lesions. Characterization of postoperative fibrosis or necrotic or cystic lesions and visualization of perineural spread in malignant parotid lesions are other conditions for which we, as well as others, have noted a potential adjunctive value for contrast-enhanced MR images (Fig 1) (6, 7, 13, 14). However, FS FSE T2 images often can provide equivalent information without the added cost and inconvenience to the patient and with significant reduction in imaging time.

In conclusion, our data suggest that optimal MR imaging of the parotid gland could be achieved by T1-weighted and fat-suppressed FSE T2-weighted sequences. Gadolinium-enhanced images should not be obtained routinely in a standard parotid MR imaging protocol. When a contrast-enhanced study is needed, fat suppression should be used, and precontrast T1-weighted images always should be obtained. Standard spin-echo T2-weighted sequences no longer should be used and should be replaced by FS FSE T2, IR FSE T2, or equivalent sequences whenever possible.

References

1. Ross MR, Schomer DF, Chappell P, Enzmann DR. MR imaging of head and neck tumors: comparison of T1-weighted contrast-enhanced fat-suppressed images with conventional T2-weighted and fast spin-echo T2-weighted images. *AJR Am J Roentgenol* 1994;163:173–178
2. Panush D, Fulbright R, Sze G, Smith RC, Constable RT. Inversion-recovery fast spin-echo MR imaging: efficacy in the evaluation of head and neck lesions. *Radiology* 1993;187:421–426
3. Yousem DM, Montone KT, Sheppard LM, Rao VM, Weinstein GS, Hayden RE. Head and neck neoplasms: magnetization transfer imaging. *Radiology* 1994;192:703–707
4. Vogl TJ, Mack MG, Juergens M, et al. MR diagnosis of head and neck tumors: comparison of contrast enhancement with triple-dose gadodiamide and standard-dose gadopentate dimeglumine in the same patients. *AJR Am J Roentgenol* 1994;163:425–432
5. Joe VQ, Westesson PL. Tumors of the parotid gland: MR imaging characteristics of various histologic types. *AJR Am J Roentgenol* 1994;163:433–438
6. Barakos JA. Advances in magnetic resonance imaging of the head and neck. *Top Magn Reson Imaging* 1994;6:155–165
7. Takashima S, Noguchi Y, Okumura T, Aruga H, Kobayashi T. Dynamic MR imaging in the head and neck. *Radiology* 1993;189: 813–821
8. Tien RD, Hesselink JR, Szumowski J. Improved detection and delineation of head and neck lesions with fat suppression spin-echo MR imaging. *AJNR Am J Neuroradiol* 1991;12:19–24
9. Lufkin RB, Hanfee W. MRI of the head and neck. *Magn Reson Imaging* 1988;6:69–88
10. Tien RD, Hesselink JR, Szumowski J. Improved detection and delineation of head and neck lesions with fat-suppression spin-echo MR imaging. *AJNR Am J Neuroradiol* 1991;12:19–24
11. Zoarski GH, Mackey JK, Anzai Y, et al. Head and neck: initial clinical experience with fast spin-echo imaging. *Radiology* 1993; 188:323–328
12. Chaudhuri R, Bingham JB, Crossman J, Gleeson MJ. MR imaging of the parotid gland using the STIR sequence and gadolinium-enhanced imaging. *Clin Otolaryngol* 1992;17:211–217
13. Sigal R, Monnet O, Baere Td, et al. Adenoid cystic carcinoma of the head and neck: evaluation with MR imaging and clinical-pathologic correlation in 27 patients. *Radiology* 1992;184:95–101
14. Vogl TJ, Dresel SH, Spath M, Grevers G, Schedel HK, Lissner J. Parotid gland: plain and gadolinium-enhanced MR imaging. *Radiology* 1990;177:667–674
15. Tien RD. Fat-suppression MR imaging in neuroradiology: techniques and clinical application. *AJR Am J Roentgenol* 1992;158: 369–379
16. Catasca JV, Mirowitz SA. T2-weighted MR imaging of the abdomen: fast spin-echo vs conventional spin-echo sequences. *AJR Am J Roentgenol* 1994;162:61–67
17. Low RN, Francis IR, Sigeti JS, Foo TKF. Abdominal MR imaging: comparison of T2-weighted fast and conventional spin-echo, and contrast enhanced fast multiplanar spoiled gradient-recalled imaging. *Radiology* 1993;186:803–811

18. Constable RT, Smith RC, Gore JC. Signal-to-noise and contrast in fast spin echo (FSE) and inversion-recovery FSE imaging. *J Comput Assist Tomogr* 1992;16:41–47
19. Jolesz FA, Higuchi N, Oshio K, et al. Clinical implementation of fast spin-echo imaging. *Radiology* 1991;181:164–165
20. Jones KM, Mulkern RV, Schwartz RB, et al. Fast spin-echo MR imaging of the brain and spine: current concepts. *AJR Am J Roentgenol* 1992;158:1313–1320
21. Mirowitz SA. Fast scanning and fat-suppression MR imaging of musculoskeletal disorders. *AJR Am J Roentgenol* 1993;161:1147
22. Nghiem HV, Herkens RJ, Francis IR, et al. The pelvis: T2-weighted fast spin-echo MR imaging. *Radiology* 1992;185:213–217
23. Fulbright R, Panush D, Sze G, Smith RC, Constable RT. MR of the head and neck: comparison of fast spin-echo and conventional spin-echo sequences. *AJNR Am J Neuroradiol* 1994;15:767–773
24. Barakos JA. Orbit, skull base, and pharynx: contrast-enhanced fat suppression MR imaging. *Radiology* 1991;179:191–198
25. Anzai Y, Lufkin RB, Jabour BA, Hanafee WN. Fat suppression failure artifacts simulating pathology on frequency-selective fat-suppression MR images of the head and neck. *AJNR Am J Neuroradiol* 1992;13:879–884